

Kirigami Skin Improves Soft Earthworm Robot Anchoring and Locomotion Under Cohesive Soil

Bangyuan Liu¹, Yasemin Ozkan-Aydin², Daniel I. Goldman², and Frank L. Hammond III¹

Abstract—Earthworms can move beneath soil by expanding parts of their bodies radially; bristles called setae work as anchors during surface locomotion but their efficacy during subsurface movement is unknown. We designed a soft, worm-like robot which models the putative earthworm anchoring mechanisms by combining Kirigami skin with radially-expanding pneumatic actuators. The robot consists of three pneumatic actuator segments: head and tail segments that expand radially as anchors, and a middle segment that elongates the body. The Kirigami structure pops up when an actuator is radially expanded, forming bristle-like spikes which are perpendicular to surface, and folds back down when deflated, forming a smoother skin structure. The robustness of Kirigami skin is improved by introducing a novel silicone-plastic layer fabrication method. The pop-up features penetrate the soil without significantly deforming the soil surface, improving the anchoring ability of the segment. Improvements in anchoring are studied systematically by measuring the differences in segment drag forces beneath soil. The performance of robot locomotion in soil terrain with or without Kirigami skin was measured in several terrain conditions (within a cohesive garden soil channel, buried in cohesive soil) as the robot dragged payloads behind it. The Kirigami skin-covered robot exhibits a greater maximum drag force (improved from $2.1 \pm 0.3\text{N}$ to $5.5 \pm 0.5\text{N}$ in 25mm hole diameter condition), greater forward displacement, and higher traction (e.g., with an 40g payload, the $3.7 \pm 2.8\text{cm}$ improved to a $12.5 \pm 0.1\text{cm}$ in 6 gait cycles).

I. INTRODUCTION

Earthworms locomote through the soil by coordinated contraction of their circular and longitudinal muscles in a motion called retrograde peristalsis, where the movement of the contractile wave flows opposite the direction of locomotion [1]. To move forward, the earthworm must be able to push against the burrow walls, anchoring itself by expanding segments of its body radially (Fig. 1-a-b). Earthworm bristles, called setae, extend when the longitudinal muscles are contracted (Fig. 1-c). Setae are known to improve anchoring during surface locomotion, but their efficacy during subsurface movement is still unknown. In this paper, we designed a soft, burrowing robot which can locomote in soil. The robot models the aforementioned putative earthworm anchoring mechanisms by combining Kirigami skin with radially-expanding pneumatic actuators (Fig. 1-d).

*This work is supported by NSF Grant No. 1545287 and IRIM seed grant program at the Georgia Institute of Technology.

¹Bangyuan Liu and F. L. Hammond III are with the Woodruff School of Mechanical Engineering at the Georgia Institute of Technology, 313 Ferst Drive NW, Atlanta, GA 30332. bangyuanliu1@gmail.com, frank.hammond@me.gatech.edu

²Yasemin Ozkan-Aydin and Daniel I. Goldman with the School of Physics, Georgia Institute of Technology, GA, USA. yasemin.ozkanaydin@physics.gatech.edu, daniel.goldman@physics.gatech.edu

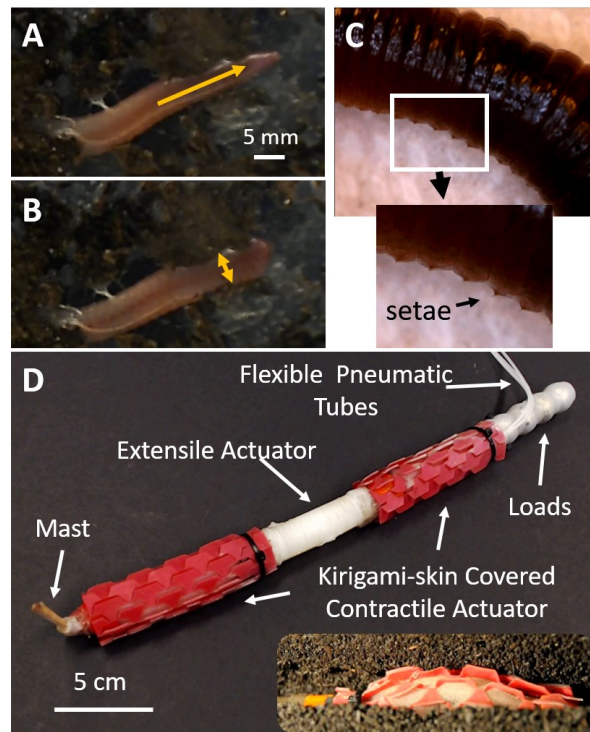


Fig. 1. Earthworm locomotion in different environments and soft earthworm robot with Kirigami skin. (a) Elongation of the anterior part in garden soil. (b) The earthworm anchors its front part to the burrow. (c) A close-up of the earthworm setae that appear when the longitudinal muscles are contracted. (d) Soft Earthworm Robot with loads (sphere balls, 20g/per each) attached to tail. The right bottom shows anchoring of Kirigami-skin covered robot contractile actuator in soil.

Earthworm locomotion has been studied by many researchers, and several earthworm-like robots were made based on it. Menciassi et al. designed an earthworm robot which replicates the radial expansion of earthworm body by actuating shape memory alloy (SMA) contrasting a silicone shell [2]. Kim et al. mimics the earthworm's locomotive and its setae clamping mechanism by using SMA for body contraction, and micro needle as fixed 'setae' [3]. Omori et al. developed a peristaltic robot which increases body radius by actuating servomotor to contract body, which forces rubber sheets attached to body to bend outward [4]. Saito et al. designed an earthworm robot with SMA and braided tube. The braided tube is contracted by SMA which increases self diameter [5]. Seok et al. built a peristaltic soft robot with sequential antagonistic motion by utilizing flexible braided mesh-tube structure actuated by a SMA

spring actuator (nickel titanium (NiTi) coil actuators) [6]. Chowdhury et al. built a earthworm-like modular robot using double crank mechanism to realize body friction modulation for peristaltic locomotion [7]. Luo et al. designed a earthworm robot by utilizing scissor mechanisms for body radius change [8]. Fang et al. presented a earthworm robot design by utilizing origami ball structure, which is actuated by servomotor and would radially expanded when axially shortened [9]. Inspired by earthworm, Ge et al. developed a soft crawling robot which changes body friction by inflating soft pneumatic actuator to attach ground [10]. Kamata et al. designed a narrow pipe inspection robot by mimicking earthworm peristaltic locomotion. The robot's straight-fibre artificial muscle expands in the radial direction when inflated [11]. Patil et al. designed a peristaltic soft robot using SMA actuators with braided tube [12]. Aydin et al. designed a multi-segmented soft worm robot which acts as a simplified robophysical model of an earthworm [13].

These papers replicate earthworm-like peristaltic motion via various mechanisms of radial actuator expansion and friction control. However, all the aforementioned earthworm-like robots were only studied and tested above ground or in a rigid fixed tube. There is an intrinsic difference between soil terrain and experimental rigid fixed terrain: namely, that the former can be modified during robot-environment interaction, which makes it harder to anchor. Current robotic anchoring mechanisms are not designed for soil terrain. The anchor mechanism for soil terrain needs to be studied, since it is essential to both real earthworm and earthworm robot motion in non-artificial terrain. Radial expansion for anchoring can be realized by using single soft contractile actuator. However, if the radial expansion is insufficient to produce the required traction, sliding can occur at the anchor points, reducing forward motion. Kirigami is a 2D layer structure cut into certain patterns, which transform into 3D structure when strain is applied, inducing buckling.

Rafsanjani et al designed a crawler robot covered by Kirigami skin, which produces anisotropic friction when kirigami features pop up, enabling the robot to crawl in a single direction above-ground [14]. Since this Kirigami skin pattern is only stretchable in a certain direction while non-stretchable in the orthogonal direction, it is especially designed for extensile actuators, which does not fit the contractile actuators used for burrowing robots. Inspired by earthworm setae and Kirigami skin, we designed a Kirigami skin especially for contractile actuators. The Kirigami skin structures pop up spike-like 'setae' when the actuator expands radially. Additionally, we improved the robustness of Kirigami skin by introducing a novel silicone-plastic layer fabrication method. With Kirigami skin, the anchoring ability of actuator can go beyond its limits. Besides, during anchor process, spike-like 'setae' of Kirigami skin can provide enough traction while making less disturbance on the terrain surface (material should be cohesive) compared to same size (when inflated) bare actuator, which can improve the next cycle's gait performance.

II. FABRICATION OF SOFT EARTHWORM ROBOT WITH KIRIGAMI SKIN

In this section, we will describe the fabrication steps of a pneumatically actuated earthworm robot that will be used for the systematic testing of Kirigami skin. Besides, we designed a new Kirigami skin fabrication method which greatly improve its robustness. To generate peristaltic motion, the robot needs at least three individually actuated segments; two radially-expanding actuators at each ends for anchoring and one longitudinally-expanding actuator at the center for elongation along the direction of locomotion.

A. Robot Fabrication

The 65 mm cylindrical extensile chamber, with outer diameter of 20 mm and thickness of 1.5 mm, were cast with DragonSkin10 NV silicone (Smooth-On, Inc.) in 3D-printed molds (uPrint SE Plus, Stratasys, Ltd.) around cylindrical metal plugs ($d=17$ mm). After the first layer was cured, Kevlar thread was wrapped around the cylinder in double-helical fashion at a pitch of 2mm to constrain expansion to the longitudinal axis. The second layer (1.5 mm) of same silicone was used to encapsulate Kevlar thread wrapping and fill the air holes resulting from the fabrication error of the first step molding. To make the actuator air tight both ends were also sealed with silicone with 5 mm in thickness (Fig. 2).

The contractile actuators (thickness 3 mm) are built in a same way of the extensile actuator without Kevlar thread. The contractile actuators can both extend longitudinally and radially depending on the pressure around the body. The three segments connected to each other by press-fit rigid rings, and very flexible tygon tubes are routed inside the actuators. We used conic shape 3D printed rigid nose to reduce the resistant force in the direction of locomotion. The CAD diagram of the final assembly is given in Fig. 2-g.

The earthworm robot is actuated pneumatically by using the air from a stationary source which transferred by a

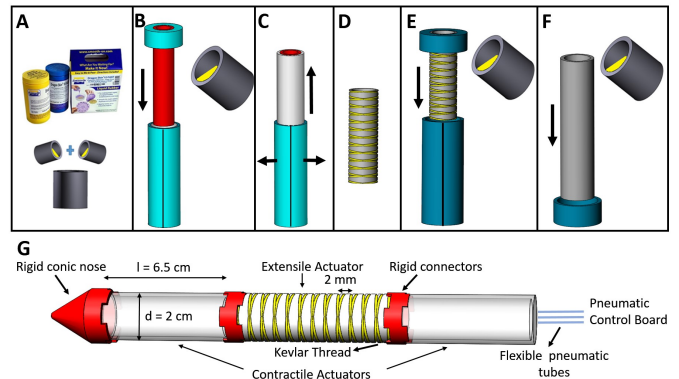


Fig. 2. Soft earthworm robot fabrication steps. (a) Mixing of the two part silicone, (b) Molding of the first layer (c)-(d) Demolding first layer and wrapping Kevlar thread. Depending on the actuator type the angle and type of the wrapping can change [15]. (e)-(f) Molding the second layer and caps. (g) The fabricated robot has three silicone segments (one extensile at the middle and two contractile at the ends) connected by rigid rings and a conically shape nose. The flexible pneumatic tubes are connected to the control board given in Fig. 3.

pneumatic control board. The inflation and deflation of each actuator are controlled by 5-port solenoid valves. The mode of solenoid valves are decided by an Arduino Due controller according to the gait program and controlled by high speed MOSFETs switches. The inflation amount are controlled by pneumatic regulators individually. The pneumatic control board is given in Fig. 3.

B. Kirigami Skin Fabrication

The design of Kirigami skin is based on previous work. [14] Due to the Kirigami skin structure's feature, it can be stretched easily in a certain direction while non-stretchable in the orthogonal direction. (in Fig. 4-D, stretchable in vertical direction, non-stretchable in horizontal direction.) In order to fit the contractile actuator's radius expansion deformation, we change the assembly direction 90 degrees compared to previous work. In order to maximize the performance of Kirigami skin pop-up features for anchoring without breaking itself, we also designed a new fabrication method to improve the Kirigami skin's robustness by combining single polyester plastic sheet with silicone membrane.

For fabrication, the polyester plastic sheet (Artus Corporation, NJ) is cut in a 100mm*100mm size and attached to the bottom of mold, which is a square groove with 110mm side length and 1.5mm in depth. Then the mold is cast with mixed DragonSkin10 NV silicone (Smooth-On, Inc.). Excess material is scraped off by a bar, leaving 1mm of silicone in the mold. After the silicone is cured, a silicone-plastic combined membrane with 1mm thickness forms and is cut into the Kirigami shape pattern by a laser cutter (Universal). The process of laser cutting repeats 3-4 times with a setting of low power and speed (30% power, 20% speed) to make sure the membrane is cut thoroughly without damaging Kirigami hinge features. Then the membrane with the Kirigami pattern is rolled up as a hollow cylinder, 20mm in diameter, with the stretchable direction being along the circumference. The plastic side of the membrane surface is rolled up inside while the silicone side is outside, in order to increase the interaction force with environment. The top

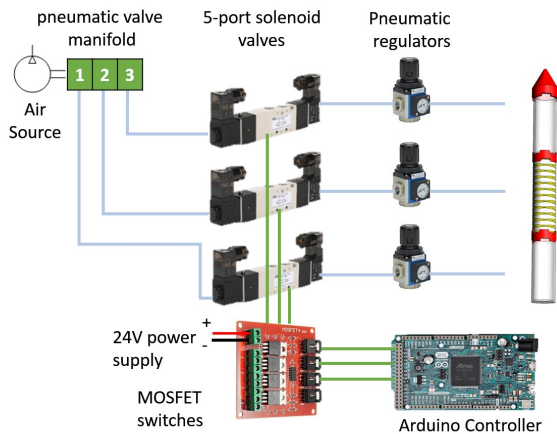


Fig. 3. Pneumatic control board that includes 5-port solenoid valves, pneumatic regulators, high speed MOSFETs and an Arduino Duo controller.

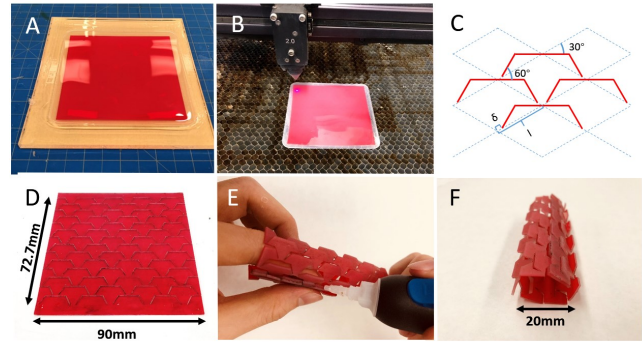


Fig. 4. Silicone-plastic Kirigami skin fabrication steps. (a) Cut 10cm*10cm polyester plastic sheet and attach to the bottom of mold. Fill the mixed silicone gel. (b) Demolding the silicone-plastic combined membrane and cut the Kirigami pattern via Laser cutter. (c) The shape of trapezoidal Kirigami cutting pattern. (d) The trapezoidal pattern silicone-plastic Kirigami membrane. (e) Glue the top row to the bottom row with plastic side inside, silicone side outside. (f) Finished Silicone-plastic Kirigami skin.

row of Kirigami unit cell is glued to the bottom row by using super glue (Loctite). The fabrication of Kirigami skin is given in Fig. 4.

For the Kirigami pattern, we tested with several Kirigami patterns and choose the most flexible and stretchable design pattern, the trapezoidal pattern. Besides, the Kirigami unit cell size also influences anchoring performance. Besides, the pop-up features should not be too small or too big, otherwise it will not be able to insert into soil deeply as anchor, or will not pop-up successfully due to external resistance torque from environment. We tested several sizes and choose the Kirigami skin unit cell with parameter of $l = 6\sqrt{3}\text{mm}$, $\delta/l = 0.16$, where l is triangular lattice unit cell hypotenuse length, δ is the hinge width along hypotenuse (Fig. 4-C).[14] For a single Kirigami skin includes 5×14 of unit cell. What's more, the thickness polyester plastic sheet should not be too small or too big, otherwise the Kirigami pop-up structure will not be strong enough to withstand external resistance, or will required a greater pressure to actuate the segment pop-up. We tested several polyester plastic sheet with different thickness and choose the 0.05mm one.

The robustness of the Kirigami skin is greatly improved by combining plastic sheet layer with silicone layer (silicone-plastic Kirigami). The stretching ability of silicone-plastic Kirigami skin and single plastic Kirigami skin are tested on uniaxial testing machine (Instron 5965). Fig. 5 shows the results when applying strain from 0 to 96%. In Fig. 5-A when applied strain is 96%, even some plastic parts of silicone-plastic Kirigami break, but the silicone layer can still hold the connection, with stretching force per width around 0.045N/cm, enabling the rest part popping up in a good shape (shown in white dash circle). However, the single plastic Kirigami skin breaks totally when the strain exceed a certain value, and these Kirigami pop-up features will not be able to pop up anymore. Besides the improvement of robustness, the silicone-plastic Kirigami also shows a better anchoring performance in Fig. 7-c, and the advantage of reducing structure's plastic deformation.

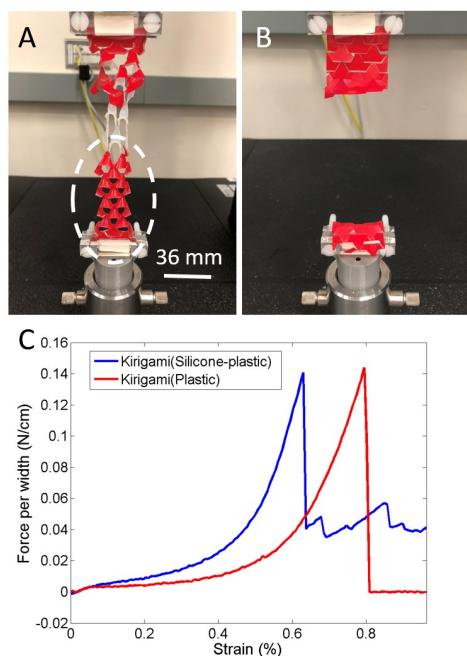


Fig. 5. Stretching test of silicone-plastic Kirigami skin. (a) 96% strain applied to silicone-plastic Kirigami skin. (b) 96% strain applied to plastic Kirigami skin. (c) Force of planar silicone-plastic Kirigami and plastic Kirigami skin (comprising 3 14 unit cells) normalized by the width (3.6cm) versus applied strain. versus applied strain for silicone-plastic Kirigami and plastic Kirigami skin.

Fig. 6-A C shows the comparison of three kinds of actuator anchoring features (the bare actuator, the plastic Kirigami skin covered actuator, and the silicone-plastic Kirigami skin covered actuator). The actuators are inflated with 30mL gas when actuated. When actuated, the outer diameter of plastic Kirigami skin covered and silicone-plastic Kirigami skin covered actuators are of the same value (36mm). This shows that the additional stress caused by the silicone layer of silicone-plastic Kirigami skin will not affect the popping-up process of Kirigami anchoring structures.

We tested the relation of pop-up level of silicone-plastic Kirigami skin covered actuator and the amount of gas inflated (or pressure). Angle θ is chosen as the description of pop up level, which is shown in Fig. 6-D. Fig. 6-E shows the result of pop-up level (θ) versus pressure when inflated by 0, 5, 10, 15, 20, 25, 30mL gas.

III. EXPERIMENTAL PROCEDURE AND RESULTS

The locomotion performance of soft earthworm robot is highly dependent on the anchoring ability of contractile actuators. With good anchoring performance in cohesive soil environment, the contractile actuators can prevent or decrease the relative slipping when anchors, dragging or pushing whole body forward more effectively. To examine the improvement made by using Kirigami skin, and the locomotion performance of soft earthworm robot, the anchoring abilities are tested by measuring the maximum drag force in cohesive soil environment, and the robot locomotion is tested within both in a soil channel and buried beneath soil.

A. Drag Force

The anchoring abilities of bare actuator, plastic Kirigami skin covered actuator, and silicone-plastic Kirigami skin covered actuator are tested by measuring the maximum drag force in a bucket of cohesive soil. The experiment equipment setup is shown in Fig. 7-a. The cohesive soil is create by mixing dry garden soil with water at a ratio of $m_{water}/m_{drysoil} = 45\%$, and the loosen mixed soil density is $0.365g/cm^3$. The compacted cohesive soil with a certain size hole at center is created by following steps: 1) erect a rod with certain diameter at the center of bucket, 2) dump same amount of loosen cohesive soil to fill the bucket, 3) compress the soil to same level by using round board, 4) remove the rod carefully. After compaction, the soil density is $0.446g/cm^3$, the depth is 113.2mm, which is longer than actuator length (65mm), and the inner diameter of bucket is 145mm which is much wider than actuator diameter (2mm). After soil environment settled, insert the actuator vertically and inflate it with 30mL air by syringe. A non-stretchable wire hooks the value attached to actuator's top and the uniaxial testing machine (Instron 5965) vertically and the inflation tube is fixed to the machine to eliminate disturbance. The drag force is measured and recorded by uniaxial testing machine while dragging the actuator totally out of the soil environment, with 120mm extension and speed of 200mm/min.

As an example, the drag force test result of 25mm hole diameter is given in Fig. 7-b, the drag force go up quickly and reaches the maximum value, and then goes done when relative sliding occurs. The maximum value of mean drag

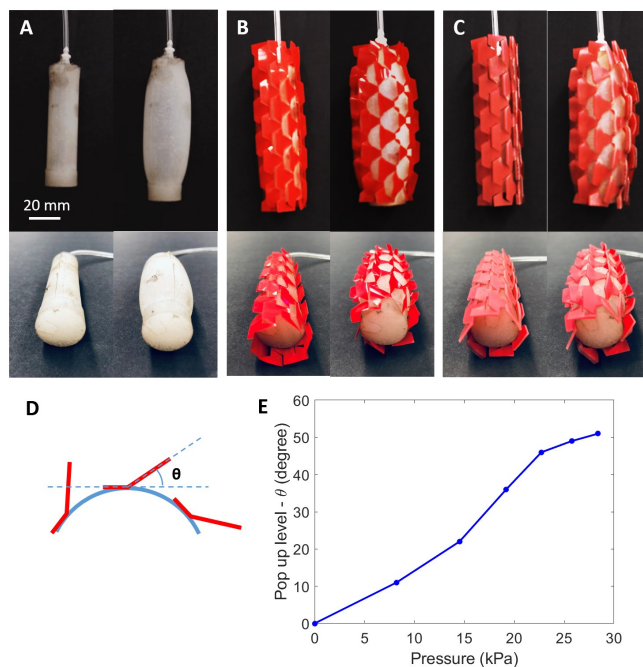


Fig. 6. The actuators features before and after actuated. (a) Bare actuator. (b) Plastic Kirigami skin covered actuator. (c) Silicone-plastic Kirigami skin covered actuator. (d) θ is the angle between Kirigami pop-up surface and tangential surface of actuator. (e) Silicone-plastic Kirigami skin covered actuator pop-up level (θ) versus pressure.

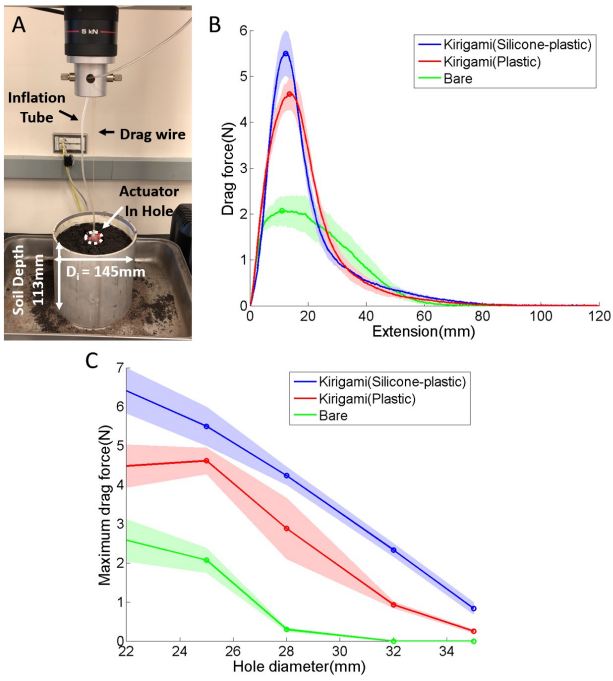


Fig. 7. Drag force experiment for actuators. (a) The experiment equipment setup. Drag force is measured by uniaxial testing machine (Instron 5965). (b) Drag force of three types actuators versus extension in 25mm hole size condition. (c) Maximum drag force of three types actuators versus different initial hole diameter.

force curve of three actuators within different diameter holes are given in Fig. 7-c. The result shows anchoring ability improvement with the help of Kirigami skin. Also, silicone-plastic Kirigami skin performs better in anchoring ability than plastic Kirigami, which may be caused by the thickness and rigidity increment of pop-up anchoring structures.

B. Locomotion

The peristaltic locomotion gait pattern is given in Fig. 8. The gait cycle starts with 1) anchoring the robot tail, 2) elongating the middle segment, 3) anchoring the head while releasing the tail, 4) releasing the middle segment, and then returns to step 1. The cycle ends with all segments released.

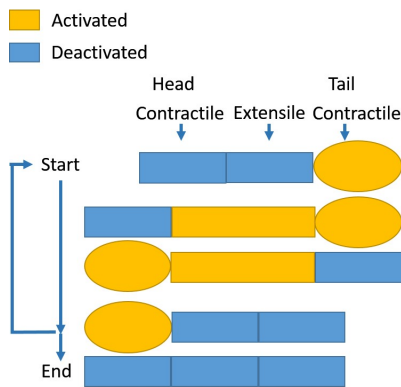


Fig. 8. Peristaltic locomotion gait pattern. The head and tail segments are contractile actuators and the middle segment is extensile actuator.

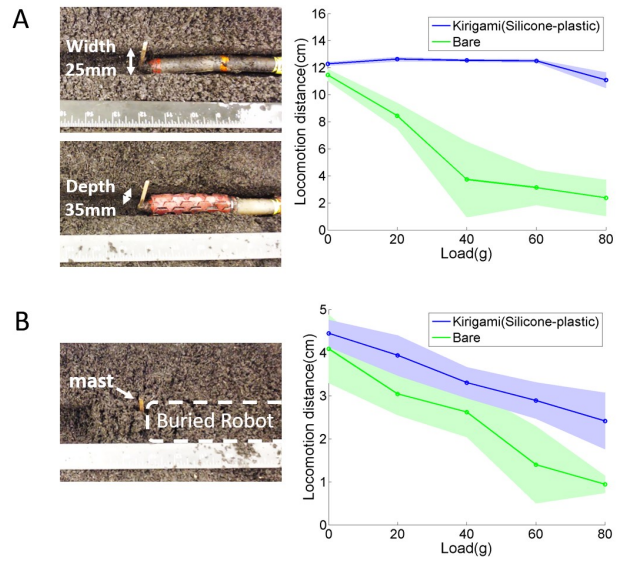


Fig. 9. Locomotion test of bare robot and silicone-plastic Kirigami skin covered robot (a) Left: Within a compacted soil channel, the size of channel is 25mm in width, 35mm in depth. Right: locomotion displacement after 6 gait cycles in soil channel terrain, with different payloads. (b) Left: Buried beneath loosen soil. Right: locomotion displacement after 6 gait cycles in soil buried terrain, with different payloads.

The locomotion and traction performance of silicone-plastic Kirigami skin covered and bare soft earthworm robots are tested and compared in two types of soil terrains as the robot dragged payloads behind it. The soil terrains includes within compacted soil channel and buried beneath loosen soil. The loosened and compacted soil conditions are the same as in the drag force test, and the channel size is 25mm in width and 35mm in depth. Fig. 9 shows the total locomotion displacement after 6 gait cycles. For both kinds of terrain condition, the silicone-plastic Kirigami skin covered robot performance a greater total forward displacement and higher traction. The silicone-plastic Kirigami skin covered robot performance is better compacted soil than in the loosened soil, especially when an initial hole is created.

In addition to measuring differences in drag force, another behavior resulting from locomotion performance and traction differences between Kirigami skin-covered and bare robots, within a compacted soil channel (or hole), is examined by having a close view of how anchoring actuators interact with terrain, shown in Fig. 10-(a-d). For the bare robot, the anchoring actuator presses the contacted terrain surface, leaving a hollow space with smooth surface feature, which can decrease the anchoring performance for next round. On the contrary, the spike-like pop-up features of Kirigami skin covered actuator inserted into soil as anchors, increasing the drag force while deforming the terrain surface structure in a smaller scale, ensuring the good performance of anchoring for next round. Such spike-like features work better when soil is compacted and cohesive. Fig. 10-e shows robot displacement after each cycle when moving within soil channel with 40g payload, which is an example caused by mechanism illustrated above. The bare robot's anchoring and

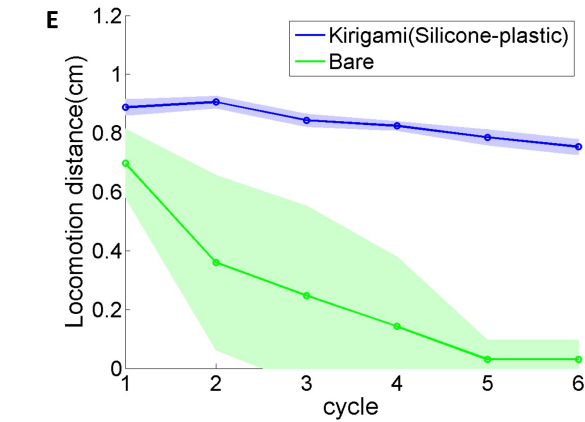
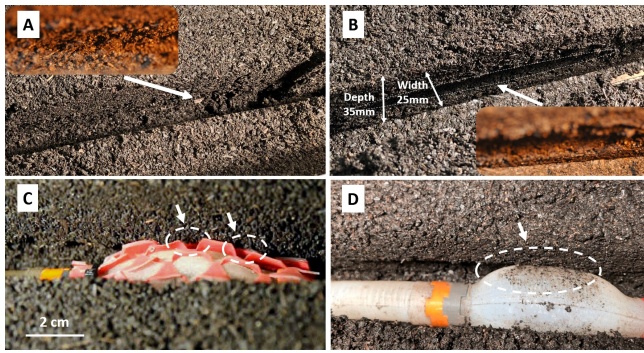


Fig. 10. Robot moving in a hole with the Kirigami skin. The disturbances generated by the robot while moving in a predefined ditch (a) with and (b) without Kirigami skin. (c) shows how Kirigami skin pop-up structures insert into soil as anchors, circled by white dash line. (d) shows how bare actuator presses the contact soil surface, circled by white dash line, creating a smooth hollow space, which decrease the anchoring performance. (e) The displacement of each cycle within soil channel with 40g payload.

locomotion ability after each cycle decreases dramatically due to the terrain surface deformation, while the Kirigami-covered robot's decreases only slightly.

IV. CONCLUSIONS

We designed a soft earthworm robot which models the putative earthworm anchoring mechanisms by combining Kirigami skin with radially-expanding pneumatic actuators. We improved the robustness and the drag force performance of Kirigami skin by combining silicone layer with plastic sheet. Compared to a bare earthworm robot, the silicone-plastic Kirigami skin-covered robot exhibits a greater maximum drag force, greater forward displacement per gait cycle, and higher traction in cohesive soil terrain. The performance of the silicone-plastic Kirigami skin covered robot improves when the soil is compacted, due the setae-like surface features. Future works will include redesigning the Kirigami skin pattern to improve anchoring performance, reducing the impact when soil fall into the gap between Kirigami skin and actuator, and developing soft earthworm robot which is able to autonomously transition from terrain surface locomotion to burrowing.

ACKNOWLEDGMENT

This material is based upon work supported by the National Science Foundation under Grant No. 1545287. Any opinions, findings, and conclusions or recommendations expressed in this material are those of the author(s) and do not necessarily reflect the views of the National Science Foundation. We also would like to thank the Georgia Tech IRIM Seed Grant program for supporting this research.

REFERENCES

- [1] E. R. Trueman, *Locomotion of soft-bodied animals*. Edward Arnold, 1975.
- [2] A. Menciassi, S. Gorini, G. Pernorio, and P. Dario, "A sma actuated artificial earthworm," in *IEEE International Conference on Robotics and Automation, 2004. Proceedings. ICRA'04. 2004*, vol. 4. IEEE, 2004, pp. 3282–3287.
- [3] B. Kim, M. G. Lee, Y. P. Lee, Y. Kim, and G. Lee, "An earthworm-like micro robot using shape memory alloy actuator," *Sensors and Actuators A: Physical*, vol. 125, no. 2, pp. 429–437, 2006.
- [4] H. Omori, T. Hayakawa, and T. Nakamura, "Locomotion and turning patterns of a peristaltic crawling earthworm robot composed of flexible units," in *Intelligent Robots and Systems, 2008. IROS 2008. IEEE/RSJ International Conference on*. IEEE, 2008, pp. 1630–1635.
- [5] T. Saito, T. Kagiwada, and H. Harada, "Development of an earthworm robot with a shape memory alloy and braided tube," *Advanced Robotics*, vol. 23, no. 12-13, pp. 1743–1760, 2009.
- [6] S. Seok, C. D. Onal, K.-J. Cho, R. J. Wood, D. Rus, and S. Kim, "Meshworm: a peristaltic soft robot with antagonistic nickel titanium coil actuators," *IEEE/ASME Transactions on mechatronics*, vol. 18, no. 5, pp. 1485–1497, 2013.
- [7] A. Chowdhury, S. Ansari, and S. Bhaumik, "Earthworm like modular robot using active surface gripping mechanism for peristaltic locomotion," in *Proceedings of the Advances in Robotics*. ACM, 2017, p. 54.
- [8] Y. Luo, N. Zhao, H. Wang, K. J. Kim, and Y. Shen, "Design, modeling and experimental validation of a scissor mechanisms enabled compliant modular earthworm-like robot," in *Intelligent Robots and Systems (IROS), 2017 IEEE/RSJ International Conference on*. IEEE, 2017, pp. 2421–2426.
- [9] H. Fang, Y. Zhang, and K. Wang, "An earthworm-like robot using origami-ball structures," in *Active and Passive Smart Structures and Integrated Systems 2017*, vol. 10164. International Society for Optics and Photonics, 2017, p. 1016414.
- [10] J. Z. Ge, A. Calderon, and N. O. Perez-Arancibia, "An earthworm-inspired friction-controlled soft robot capable of bidirectional locomotion," *Bioinspiration & Biomimetics*, 2018.
- [11] M. Kamata, S. Yamazaki, Y. Tanise, Y. Yamada, and T. Nakamura, "Morphological change in peristaltic crawling motion of a narrow pipe inspection robot inspired by earthworms locomotion," *Advanced Robotics*, vol. 32, no. 7, pp. 386–397, 2018.
- [12] R. Patil, N. Patra, A. Sharma, P. Kavitha, and I. APalani, "Design and development of peristaltic soft robot using shape memory alloy actuators with different control strategies," in *IOP Conference Series: Materials Science and Engineering*, vol. 390, no. 1. IOP Publishing, 2018, p. 012044.
- [13] Y. O. Aydin, J. L. Molnar, D. I. Goldman, and F. L. Hammond, "Design of a soft robophysical earthworm model," in *2018 IEEE International Conference on Soft Robotics (RoboSoft)*. IEEE, 2018, pp. 83–87.
- [14] A. Rafsanjani, Y. Zhang, B. Liu, S. M. Rubinstein, and K. Bertoldi, "Kirigami skins make a simple soft actuator crawl," *Science Robotics*, vol. 3, no. 15, 2018. [Online]. Available: <http://robotics.sciencemag.org/content/3/15/ear7555>
- [15] Z. Wang, P. Polygerinos, J. T. Overvelde, K. C. Galloway, K. Bertoldi, and C. J. Walsh, "Interaction forces of soft fiber reinforced bending actuators," *IEEE/ASME Transactions on Mechatronics*, vol. 22, no. 2, pp. 717–727, 2017.